Differences in the Physical Properties of Lipid Monolayers and Bilayers on a Spherical Solid Support

Frank M. Linseisen,* Michael Hetzer,# Thomas Brumm,§ and Thomas M. Bayerl#

*Department of Physics, University of British Columbia, Vancouver, British Columbia V6T 1Z1, Canada; #Lehrstuhl für experimentelle Physik 5, Universität Würzburg, Am Hubland, 97074 Würzburg, Germany; and §Physik Department E22, Technische Universität München, 85747 Garching, Germany

ABSTRACT A monolayer of 1,2-dipalmitoyl-d_{62}-glycero-3-phosphocholine (DPPC-d_{62}) coated onto silanized silica beads (spherical supported monolayer: SSM) is studied by ^{2}H-NMR and DSC. The results are compared with those obtained from a single bilayer on the same solid support (spherical supported vesicles: SSV) and from multilamellar vesicles (MLV). The phase transition temperature (T_m) of the SSMs is significantly higher than that of the bilayer systems and the extent of this difference depends on the lipid density in the monolayer that is determined during its preparation. ^{2}H-NMR reveals a gel and fluid phase coexistence in the SSM transition region. A comparison of the ^{2}H-NMR line shapes suggests the presence of highly curved structures for the fluid phase of the SSM samples. From a comparison of SSM and SSV transverse relaxation in the fluid phase we can conclude that the lateral diffusion coefficient D_l in supported monolayers is similar to that in bilayers.

INTRODUCTION

The Langmuir-Blodgett technique is widely used for the transfer of monomolecular films of amphiphilic molecules onto solid substrates. It is particularly useful for the preparation of phospholipid monolayers on a solid support and their study by surface sensitive techniques like ellipsometry (Cresswell, 1994; Malmsten, 1994; Geib et al., 1991), surface plasmon spectroscopy (Fischer et al., 1993; Schmitt et al., 1992; Häussling et al., 1991), evanescent field techniques (Miehlich and Gaub, 1993; Reinl and Bayerl, 1993; Okamura et al., 1990) and scanning force microscopy (Putman et al., 1992; Zasadzinski et al., 1994a,b).

These techniques, together with the classical film balance and fluorescence methods (Thomas and Möhwald, 1994; Möhwald, 1990; Fischer and Sackmann, 1986; Lösche et al., 1983) and the more recent application of x-ray, synchrotron (Möhwald, 1993; Helm et al., 1987), and neutron reflection (Brumm et al., 1994; Johnson et al., 1991; Vaknin et al., 1991) techniques have provided detailed information about the physical properties of phospholipid monolayers. This, in turn, is essential for the understanding of the basic processes that account for the self-assembly, the short- and long-range order, and the superstructure formation in these two-dimensional systems.

From the viewpoint of membrane biophysics, monolayers can be considered as a simple structural model of one leaflet of a lipid bilayer, the basic structure of every biological membrane. Moreover, the hydrophilic side of a lipid monolayer can, to a certain extent, mimic the surface of a membrane with respect to the adsorption of water-soluble proteins. Therefore, many studies were devoted to the interaction of monolayers with other membrane components like proteins and steroids.

However, most information that has been gathered on monolayers is essentially structural in nature. Monolayers are quite elusive systems regarding the application of time-resolving methods like solid-state NMR that can provide information on their dynamics. This is mainly due to the comparatively low sensitivity of such methods requiring considerable amounts of phospholipids (e.g., a minimum of a few milligrams for ^{2}H-NMR) and to the probe geometry that does not allow the study of monolayers on a planar support. On the other side, ^{2}H-NMR could provide unique insight not only into the dynamics of monolayers but also into their molecular order over very short distances comparable to that of a carbon-hydrogen bond length. This would contribute to a better assessment of similarities and distinct differences between monolayers and bilayers on a molecular scale.

Our approach to making monolayers suitable for ^{2}H-NMR studies is the use of spherical silica beads of submicron dimensions and to coat them with a monolayer of chain-perdeuterated DPPC-d_{62} after appropriate hydrophobization of the silica surface. The beads provide a total surface area large enough to pack ~5–10 mg DPPC-d_{62} as supported monolayer in excess water into the 1-ml NMR sample tubes, which is sufficient for ^{2}H-NMR measurements. The use of the same silica beads for the preparation of supported bilayers enables now a very sensitive comparison of the molecular order parameter profile and the relaxation behavior of monolayers and bilayers.

MATERIALS AND METHODS

Materials

1,2-dipalmitoyl-d-$_{62}$-sn-glycero-3-phosphocholine (DPPC-d_{62}) was purchased from Avanti Polar Lipids Inc. (Birmingham, AL) and used without

Received for publication 15 May 1996 and in final form 16 January 1997.

Address reprint requests to Dr. Thomas Bayerl, Lehrstuhl für experimentelle Physik 5, Universität Würzburg, Am Hubland, 97074 Würzburg, Germany. Tel.: 011-49-931-888-5863; Fax: 011-49-931-888-5851; E-mail: tbayerl@physik.tu-muenchen.de.

0006-3495/97/04/1659/09 $2.00

further purification. *N*-2-Hydroxyethylpiperazine-*N'*-2-ethanesulfonic acid (HEPES) was obtained from Sigma Chemical Co. (St. Louis, MO) and Octadecyl-di-methyl-mono-chlorosilane (OMS) from ABCR GmbH & Co. (Karlsruhe, Germany). Silica beads (KUSI) were kindly provided by Dr. Meyer from Degussa AG Anorganic Chemistry Research (Hanau, Germany). Electron microscopy showed the beads to be perfectly spherical with a diameter of 400 ± 60 nm.

Preparation of bilayer vesicles

The multilamellar vesicle (MLV) sample was prepared by vortexing 44.7 mg DPPC-d_{62} above its phase transition temperature of 37.5°C in 0.6 ml deuterium-depleted water (50 mM HEPES buffer at pH = 7.0). The sample was pipetted into a 10 mm plastic NMR sample tube and stored at −30°C.

The solid supported vesicle (SSV) sample was prepared according to a previously described procedure (Bayerl and Bloom, 1990; Naumann et al., 1992). 600 mg KUSI were coated >40°C with ~13 mg lipid. 50 mM HEPES buffer at pH = 7.0, denoted buffer *A*, was used for all washing steps and in the last two, the water in buffer *A* was substituted by deuterium-depleted water. The sample was transferred into a 10-mm plastic NMR tube and stored at +4°C.

Preparation of supported monolayers

The basic idea for the preparation of the solid supported monolayer (SSM) sample is to use a hydrophobic carrier material, in our case KUSI, silanized with OMS. The transfer of the lipid onto these hydrophobic KUSI was achieved by dissolving the lipid in a nonpolar solvent containing the silanized KUSI and successively increasing the solvent polarity.

The preparation of the bonded hydrocarbon phase was performed similarly to methods described in Hennion et al. (1978) and Kirkland (1975). About 5 g KUSI were sonicated for 2 min. in 1 M sulfuric acid to obtain the maximum number of reactive surface silanol groups. The beads were washed in distilled water to neutrality (~6 times) by repeated sonication, centrifugation, removal of the supernatant, and resuspension. One additional washing step was carried out in methanol before drying for 12 h at 190°C under vacuum. 5 g KUSI (28 m^2 surface area), containing approximately one silanol group per 20 $Å^2$ (Wasserman et al., 1989b), were placed in a 100-ml round-bottom flask. 40 ml dry toluene, treated with a Type 4A molecular sieve, and 5.5 g OMS (~100-fold area excess) were added. This mixture was refluxed under constant stirring for 18 h at the temperature of boiling toluene (111°C) with a slow stream of dry nitrogen. To remove unbonded OMS the silanized KUSI were washed six times by centrifugation and resuspension in HPLC grade methylene chloride. The silanized KUSI were stored in methylene chloride.

With ellipsometry and low-angle x-ray reflection Wasserman et al. (1989a,b) determined the thickness of an OTS monolayer on silica as 26 Å and the cross-sectional area per silane hydrocarbon chain as 22.5 ± 2.5 $Å^2$. An AFM study of OTS on Mica showed that the deposition of the hydrocarbon layer occurs by nucleation and growth of self-similar islands (Zasadzinski et al., 1994b), whereas on silica surfaces one observes uniform growth (Wasserman et al., 1989b). In either case, the silanized surface was smooth and free of holes.

Using a MC-2 microcalorimeter, we performed a DSC run on 0.8 g silanized KUSI suspended in 0.5 ml hexane at scan rates of 10, 30, and 60°C/h in ascending temperature mode (temperature range 10–55°C). No signatures of any phase transitions could be found. A broad-line ^{1}H-NMR measurement [similar to MacKay (1981)] of 0.8 g silanized KUSI suspended in 1 ml CCl_4, gave a value for the second moment M_2 of the proton NMR line shape of M_2 (20°C) ≥ 1.6×10^9 s^{-2}, which is similar to the second moment M_2 of DPPC-d_0 in the pretransition region of M_2(DPPC-d_0) ≈ 2×10^{-9} s^{-2} (MacKay, 1981). From the DSC and ^{1}H-NMR results, we concluded that the alkyl-chains of the silane layer have a similar-order parameter like the DPPC-d_0 in the gel-state up to temperatures of at least 55°C.

Two types of SSM samples (presumably with different lipid densities) were prepared, denoted by SSM-L and SSM-H. For each sample type, 1 g silanized KUSI (5.6 m^2 surface area) and 35 mg DPPC-d_{62} (16 m^2 monolayer area) were suspended in 30 ml methylene chloride in a 50-ml round bottom flask attached to a rotary evaporator. By heating to 35°C (40°C for SSM-H) and the application of a moderate vacuum using a water aspirator, half of the solvent was removed. The solvent level was restored to 30 ml by adding HPLC grade methanol. Again, half of the volume was evaporated and replaced by methanol. The temperature was raised to 60°C (50°C for SSM-H), half the solvent was removed, and replaced with buffer *A*. Keeping the temperature at 60°C (increasing to 60°C for SSM-H) for ~2 h the organic solvent was removed.

The lipid-coated KUSI were removed from the coating solution by centrifugation. They were washed 4 times in buffer *A* by centrifugation, discarding the supernatant and resuspension via vortexing. Two final washing steps were carried out in buffer *A* with deuterium-depleted water. The samples were transferred into 10-mm plastic NMR tubes and stored at +4°C.

From the number of washing steps and the solvent volumes exchanged at each step, one can estimate the final methanol concentration in the SSM samples being $<1.3 \times 10^{-6}$ mol/mol DPPC-d_{62}. [The molar partition coefficient of methanol in DPPC versus water is 2.3 (Rowe, 1983, 1985).] This low concentration should have negligible effects on the DSC and NMR spectra of the SSM samples, which was confirmed by using an alternative SSM preparation procedure (paper in preparation) that did not involve organic solvents at all.

Moreover, by using perdeuterated organic solvents for the SSM preparation and protonated DPPC, we were able to check the final SSM sample for traces of organic solvent using FTIR. In measuring an SSM sample in ATR mode (4000 scans at 2 cm^{-1} resolution), we detected no signals characteristic for deuterated organic solvents in the range from 1000 cm^{-1} to 3000 cm^{-1}. This result supports the above-mentioned estimate that the SSM samples contain only negligible amounts of solvent.

A crude estimate of the amount of DPPC-d_{62} in the SSM-L sample using the integral, T_2^{qe} corrected, ^{2}H-NMR signal gave a value of 5–6 mg. This value is less than the theoretically expected amount of 11 mg DPPC-d_{62} but one has to take into account the loss of beads during SSM preparation and large uncertainties in the quantification of the NMR signal intensity. Nevertheless, this may indicate that the SSM-L sample exhibits a rather low lipid density at its surface.

We studied at least two samples for each SSM sample type. Both DSC and ^{2}H-NMR gave within experimental error identical results for the samples of the same type.

NMR experiments

^{2}H-NMR measurements were performed at 42.6 MHz on a homebuilt spectrometer described elsewhere (Sternin, 1985; Davis, 1979). The spectra were obtained by applying a quadrupolar echo pulse sequence with an 8 CYCLOPS phase cycling scheme (Davis, 1983; Rance and Byrd, 1983; Davis, 1979). For each scan 2048 complex points were collected in quadrature detection mode with a dwell time of 2.0 μs and a filter bandwidth of 200 kHz. Typically 10,000 transients were averaged for the MLV and 20,000 for the SSV and SSM sample. The length of the 90° pulse was 4.0 μs, the spacing of the two 90° pulses 40 μs, and the repetition time typically 0.3 s. The sample temperature was varied between 28 and 50°C in 2°C increments using a Bruker BV-T1000 temperature controller (Bruker Instruments Inc., Billerica, MA).

All free induction decays (FIDs) were baseline corrected, phased, and Fourier transformed starting from the top of the echo. The average half moments of the ^{2}H-NMR spectra were calculated according to Davis (1983). Oriented spectra were obtained by "De-paking" (Sternin et al., 1983) from which smoothed orientational order parameter profiles were calculated (Lafleur et al., 1989).

Spin-spin relaxation time (T_2^{qe}) measurements were performed by increasing the pulse spacing in the quadrupolar echo pulse sequence and performing an exponential fit to the FID amplitude at the top of the echo

for typically 8 pulse spacings (40–240 μs). The spin-lattice relaxation time (T_1^{ir}) was determined in the same way using the inversion recovery pulse sequence and typically 5 values for the inversion delay (1–40 ms).

For selected spectra T_2^{qe} was calculated for each frequency position (so-called relaxation spectra), similar to methods described in Nezil et al. (1991). Typically, eight spectra were used for each fit, the pulse spacings of the quadrupolar echo pulse sequence ranging from 40 to 240 μs. Each FID was phased, baseline corrected, and any remaining signal in the imaginary channel was discarded before Fourier transforming (to increase the signal-to-noise ratio). The spectra were baseline corrected and smoothed by convoluting them with a binomial windowing function. For each frequency value, an average T_2^{qe} value was determined by fitting a straight line to the logarithm of the spectral amplitude for the eight pulse spacings. The T_2^{qe} spectra determined in this way are in first approximation equivalent to the T_2^{qe} spectra determined by the method described in Nezil et al. (1991). This equivalence can be easily verified by taking the first two terms of the Taylor expansion of the formula for the general time-dependence of an ^{2}H-NMR spectrum under the influence of T_2^{qe} relaxation (Nezil et al., 1991) around $t = 0$.

DSC measurements

Differential scanning calorimetry (DSC) measurements were performed with a Hart Scientific microcalorimeter (Hart Scientific, Utah, USA) at scan rates of 17, 24, and 44°C/h, both in ascending and descending temperature mode. The ^{2}H-NMR samples were used for the DSC measurements. The offset and slope were removed from the baselines of the specific heat traces. Enthalpy measurements were performed with a MC-2 microcalorimeter (Microcal, Amherst, MA) at a scan rate of 30°C/h according to procedures described previously (Naumann et al., 1992).

RESULTS

Comparison of the phase transition behavior

The basic structural differences between SSM and SSV are represented in Fig. 1.

Fig. 2 shows the specific heat traces for the MLV, SSV, and the two SSM samples (denoted as SSM-L and SSM-H in the following), both in heating and in cooling mode. Neglecting instrumental artifacts, like the high temperature shoulder at the main transition of the MLV sample heating scan, the DSC traces for heating and cooling are very similar in shape for all samples.

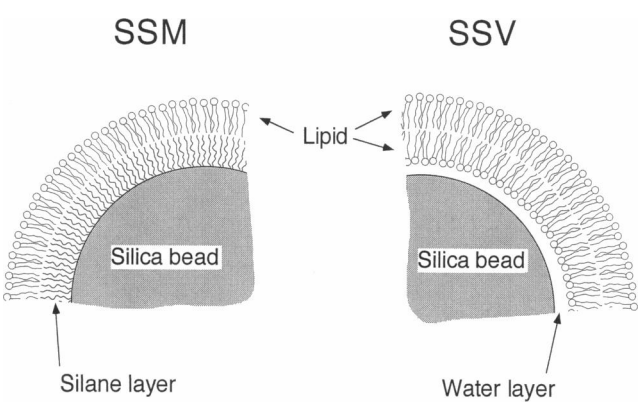

FIGURE 1 A schematic picture of the structure of the SSV and SSM samples.

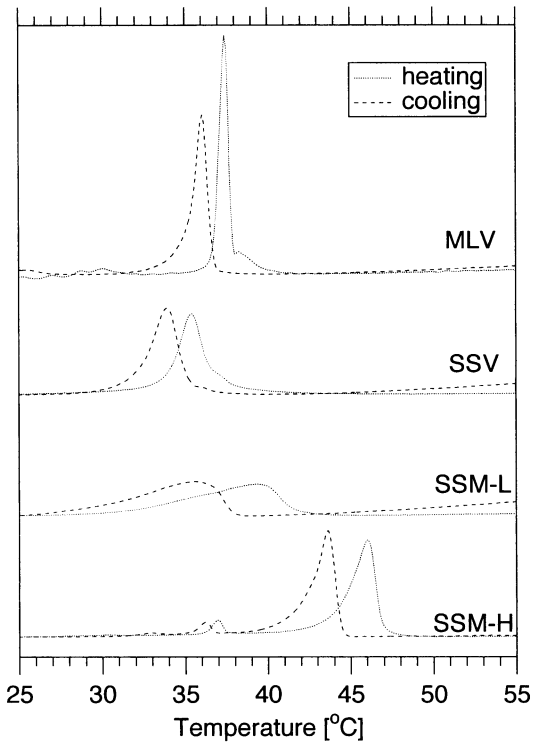

FIGURE 2 DSC traces of the MLV, SSV, and SSM samples at a scan rate of 17.0°C/h. Dotted traces were acquired in heating, dashed ones in cooling mode. Temperature shift T_{hyst} between the heating and the cooling scan: MLV, T_{hyst} = 1.3°C; SSV, T_{hyst} = 1.6°C; SSM-L, T_{hyst} = 3.7°C; SSM-H, T_{hyst} = 2.4°C.

As also described in Naumann et al. (1992), the sharp main transition of the DPPC-d_{62} MLV samples at T = 37.4°C is shifted downward in temperature by ~2.0°C to T = 35.4°C for the SSV sample. Compared to the MLV sample, the DSC peak of the SSV one shows a 1°C larger full width at half maximum (FWHM), the temperature shift between the cooling and the heating scan (denoted from here on as thermal hysteresis T_{hyst}) is increased by ΔT_{hyst} = 0.3°C (scan rate of 17°C/h) and the pretransition has disappeared.

The two SSM samples show drastic differences in their phase transitions. SSM-L exhibits a very broad asymmetric endothermic feature (FWHM = 6°C) centered at 39.3°C, while for SSM-H the transition is similar to that observed for SSV with respect to shape and symmetry. However, the SSM-H transition occurs at a much higher temperature than all other samples at 46.0°C. Also the thermal hysteresis differs between the two monolayer samples. With T_{hyst} = 3.7°C for SSM-L and T_{hyst} = 2.4°C for SSM-H, both SSM samples show higher values than the SSV sample with T_{hyst} = 1.6°C (all values for T_{hyst} were determined at a scan rate of 17.0°C/h). Hence the monolayer exhibits the highest thermal hysteresis values of all samples studied.

Whereas the shift in the peak positions with increasing scan rate (17, 24, 44°C/h) are similar for both the heating and the cooling scan for the MLV and SSV sample, the shift of the SSM-L up-scan peak is about three times larger than

for the down-scan peak. Assuming that this effect is not just due to a change in the shape of the DSC trace, the gel-to-fluid transition seems to have a slower kinetic than the fluid-to-gel one.

The enthalpy value for the SSM-L of 24 kJ/mol is within experimental error identical to the one for the SSVs (24 kJ/mol) and therefore ~25% less than for the MLVs with 31.5 kJ/mol (Naumann et al., 1992). However the SSM-L enthalpy has an error of ~±30% due to the large uncertainty in sample losses during the preparation.

Fig. 3 *a* shows a plot of the first moments M_1 of the ^{2}H-NMR spectra versus temperature for all samples studied. As in the DSC scans there is a clear signature of onset and completion of the chain-melting transition for both bilayer and monolayer samples.

As observed by DSC, the SSM-L sample shows a broad transition region (>9°C) and the values obtained for onset and completion agree well with the DSC results. A similar good agreement is obtained for the SSM-H sample.

The hysteresis in the DSC heating and cooling scans of the SSM-L sample of ~3–4°C is verified by ^{2}H-NMR by measuring M_1 (T) of SSM-L for both ascending and descending temperatures (Fig. 3 *b*). This shows that the hysteresis is not due to the kinetic limitations of the DSC measuring system. Comparing the ^{2}H-NMR spectra and the corresponding moments of the SSM samples before and after the heating/cooling cycles, we did not observe any changes. This indicates the morphological stability of the SSMs and the reversibility of the phase transition.

The values determined from the DSC and ^{2}H-NMR data are in reasonable agreement, taking into account the difficulties in determining the DSC values of the ending and starting temperatures of the phase transition. The results for the MLV and SSV sample are as reported in Naumann et al. (1992). For the SSM-L sample we have ~9°C wide gel/fluid coexistence region with its maximum shifted upward by ~3°C compared to the MLV transition. It is remarkable that the SSM-H transition occurs at an even higher temperature (9°C shift compared to MLV) and is much sharper than for SSM-L with a FWHM comparable to that of SSV.

Molecular order in monolayers and bilayers

Fig. 4 shows an overview of the spectral line shapes for the MLV, SSV, and SSM samples.

At low temperatures (left column), all samples show gel-type spectra. The large value for their first moment $M_1(T)$ of typically 1.2×10^5 s^{-1} indicates a high orientational order and the characteristic bell-shape is associated with a more restricted motion in the gel phase.

At high temperatures (right column), all samples show Pake doublet-type spectra. They have a much smaller first

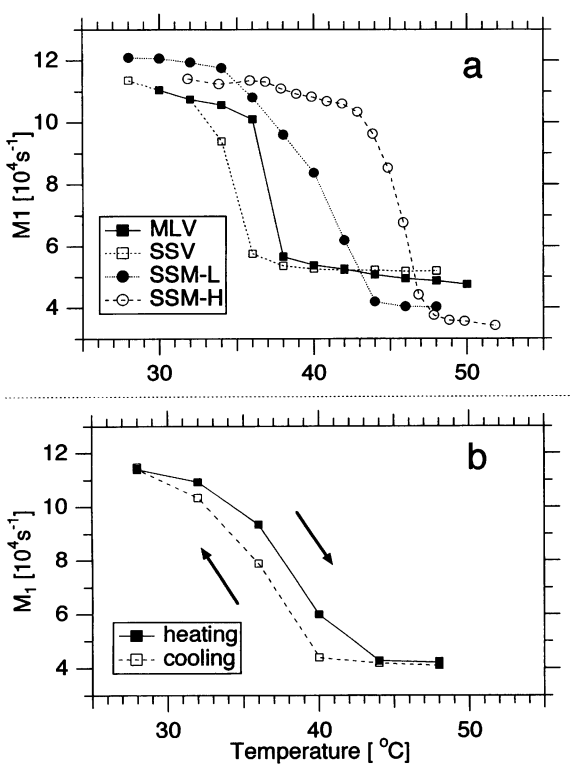

FIGURE 3 (*a*) Plot of the first moments $M_1(T)$ for the MLV, SSV, and SSM samples. (*b*) Thermal hysteresis as seen in the first moments $M_1(T)$ of the SSM-L sample. The time between successive points was 82 min.

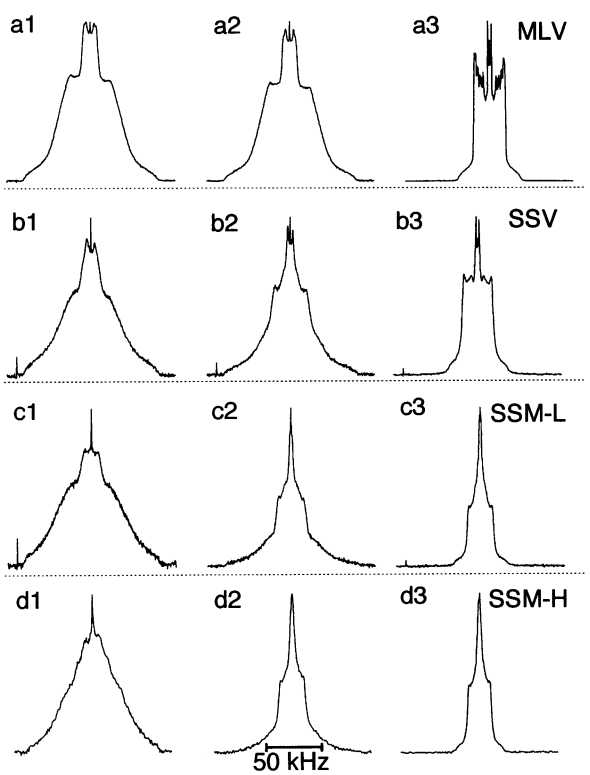

FIGURE 4 ^{2}H-NMR spectra of the MLV, SSV, and SSM samples at different temperatures. MLV (a1–a3), $T(a1)$ = 34.0°C; $T(a2)$ = 36.0°C; $T(a3)$ = 40.0°C. SSV (b1–b3), $T(b1)$ = 30.0°C; $T(b2)$ = 34.0°C; $T(b3)$ = 38.0°C. SSM-L (c1–c3), $T(c1)$ = 32.0°C; $T(c2)$ = 40.0°C; $T(c3)$ = 46.0°C. SSM-H (d1–d3), $T(d1)$ = 40.9°C; $T(d2)$ = 45.9°C; $T(d3)$ = 48.9°C.

moment M_1 of typically $\sim 5 \times 10^4$ s^{-1}, indicating the low orientational order of the acyl chains, and exhibit pronounced edges, which are caused by the axially symmetric rotation of the lipid molecules. The SSM spectra (c3 and d3) in Fig. 4 show an unusual line shape for the central part of the spectrum, resembling a pyramid in shape and being possibly caused by the superposition of a MLV type Pake doublet spectrum and a narrow spectrum (see Discussion).

As described elsewhere (Linseisen et al., 1993; Morrow et al., 1992; Huschilt et al., 1985), a gel/liquid coexistence region manifests itself in ^{2}H-NMR spectra as a superposition of gel and liquid-type ^{2}H-NMR spectra. The spectra in the middle column of Fig. 4 show signs of such a coexistence region for both the SSV and the SSM samples.

For all of our samples, at temperatures corresponding to them being in the fluid phase (see right column in Fig. 4), we calculated their oriented line shapes (Fig. 5) using a numerical algorithm called "De-Paking" (Sternin et al., 1983). The depaked spectrum of the MLV sample (Fig. 5) showed negative intensities at frequencies near the 90° orientations of the lipids with respect to the magnetic field. This is characteristic of the macroscopic orientation of the MLVs in the magnetic field of the NMR magnet (Brumm et al., 1992). The shape of the SSV depaking result, exhibiting methyl peaks with quadrupolar splittings of 4.8 and 6.8 kHz and a double peak structure for the 90° edge, which is an indication of the existence of two distinct lipid environments for the SSV sample at high temperatures. The intensity ratio of the split methyl peak gives an estimate that 30–40% of the SSV lipid exhibits lower orientational order. In a recent study (Reinl and Bayerl, 1994), it was demonstrated that such differently ordered environments are due to a nonequivalence between the inner and outer leaflet of the bilayer with respect to the silica surface.

It is noteworthy that both SSM samples, where only one leaflet (e.g., the monolayer) is present, do not exhibit such a split of methyl or methylene groups. The SSM quadrupolar splittings at the 90° edge were similar to those of the lower ordered bilayer leaflet of the SSV.

To allow for easier comparison we used the procedure described by Lafleur et al. (1989) to calculate "generalized" smoothed orientational order parameter profiles "S_{CD}" from the depaked spectra of Fig. 5. We use the term generalized order parameter profile, as the procedure used gives the "true" order parameter profile (being molecular order parameter versus position on the chain) only for the case that all the deuterium nuclei for each individual position on the chain experience the same average orientational order (e.g., no two phase coexistence region). This seems to be neither the case for the SSV sample (2 methyl splittings and double peak structure for the 90° edge) nor, as we suspect, for the SSM samples.

Although one cannot interpret the result of the procedure of Lafleur et al. (1989) as a plot of molecular order versus position on the chain for the case of spectra, which arise from the superposition of two different signals, it still holds that it gives the quadrupolar splitting (normalized to its maximum value) versus the integrated spectral intensity.

The similarity of MLV and SSV samples in their spectra line shapes on one side and of SSM-L and SSM-H ones on the other becomes clearly evident in Fig. 6. For the MLV and SSV sample we observe a plateau region for the generalized order parameters near the lipid head group/water interface, followed by a steady decrease of S toward the bilayer center.

The SSM generalized order parameter profiles show a less pronounced plateau region, followed by an almost linear decrease in order (carbon positions 7–15) toward the monolayer/silane interface.

To test the robustness of the procedure for calculating the generalized order parameter profile, we determined the influence of both a narrow signal and orientation independent

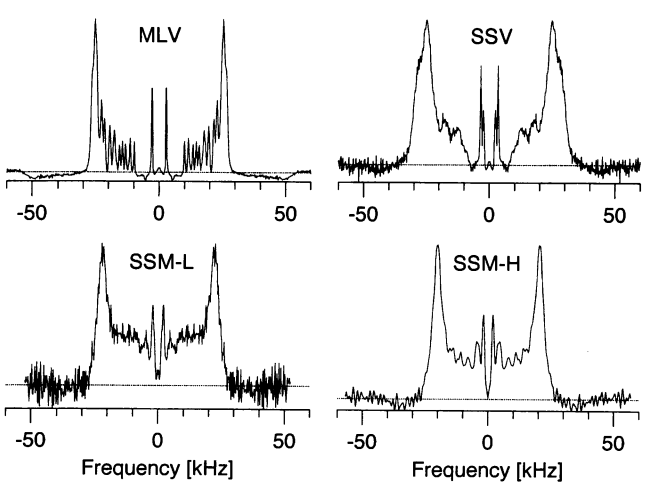

FIGURE 5 Depaked ^{2}H-NMR spectra of the MLV, SSV, and SSM samples at T = 48°C (T = 52°C for SSM-H).

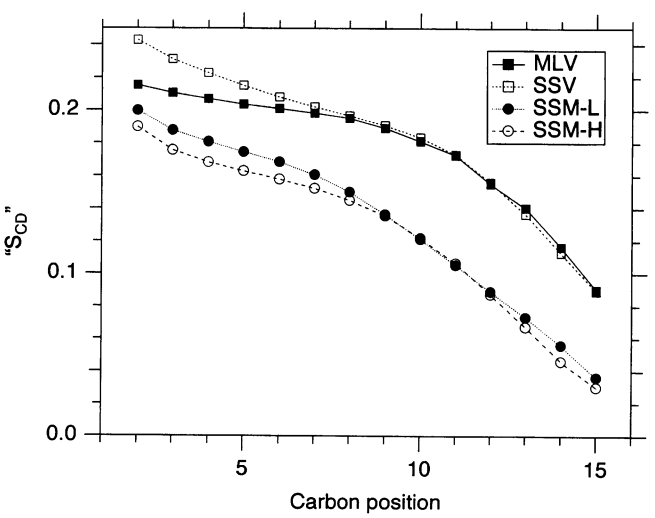

FIGURE 6 "Generalized" carbon-deuterium order parameter (see text for explanation) S_{CD} versus carbon position n along the alkyl chain for the MLV, SSV, and SSM samples at T = 48°C (T = 52°C for SSM-H).

broadening on the absolute values and the shape of the generalized smoothed order parameter profile. The error in the absolute values of the generalized order parameters, due to a narrow signal with 15% of the total intensity, was <0.004 and typically 0.001. Convolution with a Gaussian broadening function (width 4 kHz) produced changes of <0.01 and typically 0.005. Neither orientation-independent broadening nor a narrow signal produce, therefore, large changes in the values of the generalized order parameters. Furthermore, there was no noticeable change in the shape of the generalized order parameter profile for any of the above modifications.

Addressing the possibility of a distortion of the generalized order parameter profile due to relaxation effects, we recalculated the generalized order parameter profile for the SSM-L sample using data from an experiment with a longer repetition time of 1.0 s (to exclude T_1^{ir} distortions) and corrected for T_2^{qe} distortions. The T_2^{qe} correction was done by first calculating a T_2^{qe}-relaxation spectrum, and then by using these data, the absorption spectrum was extrapolated back to zero pulse spacing in the quadrupolar echo sequence. The comparison of the generalized smoothed orientational order parameter profiles from this spectrum (not shown here), being free of both T_1^{ir} and T_2^{qe} distortions, with the profile shown in Fig. 6, revealed some minor changes, but the linear decrease in generalized order between carbon positions 7–15 persisted.

An indication for a low value of the "real" molecular order parameter of the SSM deuterium atoms near the methyl group is the methyl-group ^{2}H-NMR splitting, which is ~4.0 kHz for both SSM samples compared to ~5.8 kHz for the MLV and SSV ones. It should be noted that the generalized order parameter profiles for both SSM samples were reconstructed from spectra at different temperatures (48°C for SSM-L and 52°C for SSM-H) as their T_m values differ by 5–6°C.

Monolayer and bilayer dynamics

Information on SSM dynamics was obtained by measurements of longitudinal (T_1^{ir}) and transverse (T_2^{qe}) relaxation times of DPPC-d_{62} in the three model systems.

T_1^{ir} measurements for the four samples (MLV, SSV, and SSMs) gave similar values of $T_1^{ir} \approx 50$ ms in the gel and $T_1^{ir} \approx 43$ ms in the fluid phase. The variation of T_1^{ir} with temperature is roughly sigmoidal with a steep drop of T_1^{ir} around the phase transition temperature. This similarity in T_1^{ir} indicates similar spectral densities $j(\omega_{Lamor})$ and $j(2\omega_{Lamor})$ for all samples.

The temperature dependence of T_2^{qe} is represented in Fig. 7. While the MLV sample exhibits a strong increase in T_2^{qe} at the transition temperature, T_2^{qe} is almost constant for the SSV sample and decreases steadily for both SSM samples. In the fluid phase, the T_2^{qe} values for the SSV and both SSM samples are very similar (160 ± 20 μs). It is interesting to note that both SSM samples exhibit a reversed temperature dependence in T_2^{qe} (T) as compared to the MLV one.

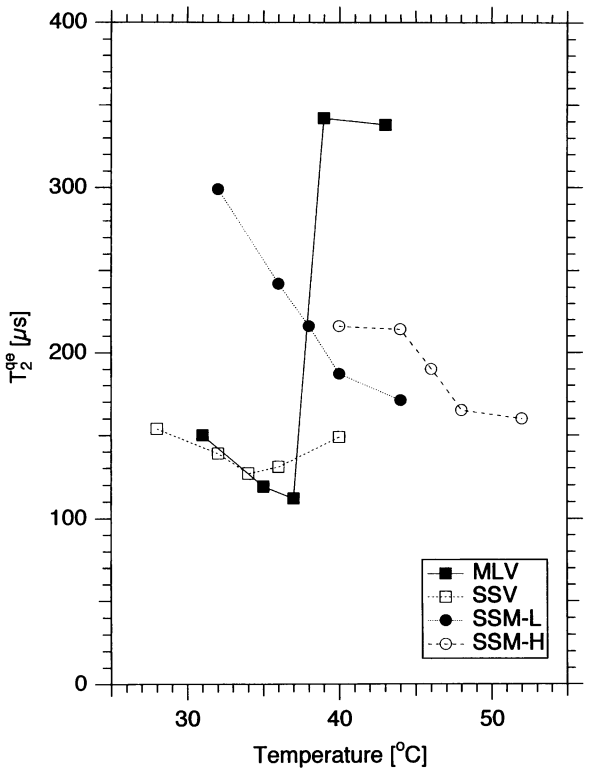

FIGURE 7 Spin-spin relaxation time $T_2^{qe}(T)$ for the MLV, SSV, SSM-L, and SSM-H sample.

The T_2^{qe} relaxation spectra (Fig. 8) show the frequency dependence of transverse relaxation of the samples. As both SSM samples gave almost identical results for both the average T_2^{qe} values and also for the relaxation spectra at temperatures corresponding to the samples being in their fluid phase (at 44°C for SSM-L and 52°C for SSM-H), only the SSM-L data are shown here. Besides the difference in the average T_2^{qe} values, which has already been discussed, the main difference between the relaxation spectra is the relative smoothness of the relaxation data for both SSMs and SSV as compared to MLV. The increase of T_2^{qe} around the 0° and 90° position in the spectrum, which is typical for systems under the influence of motions that are slow on the NMR time scale (e.g., lateral diffusion or undulations) (Bloom et al., 1992; Nezil et al., 1991) is significantly less pronounced for SSV and SSMs. The horizontal dotted lines in Fig. 8 indicate the average T_2^{qe}: 340 μs (MLV), 150 μs (SSV), and 170 μs (SSM).

DISCUSSION

In this work, we present the first DSC and ^{2}H-NMR data of phospholipid monolayers on a spherical solid support and compare them with the corresponding bilayer data. This comparison gives us confidence that our SSM are indeed monolayers and not any sort of bilayers or multilayers.

First, the DSC data and the NMR first moments clearly show that the phase transition behavior of the SSMs with

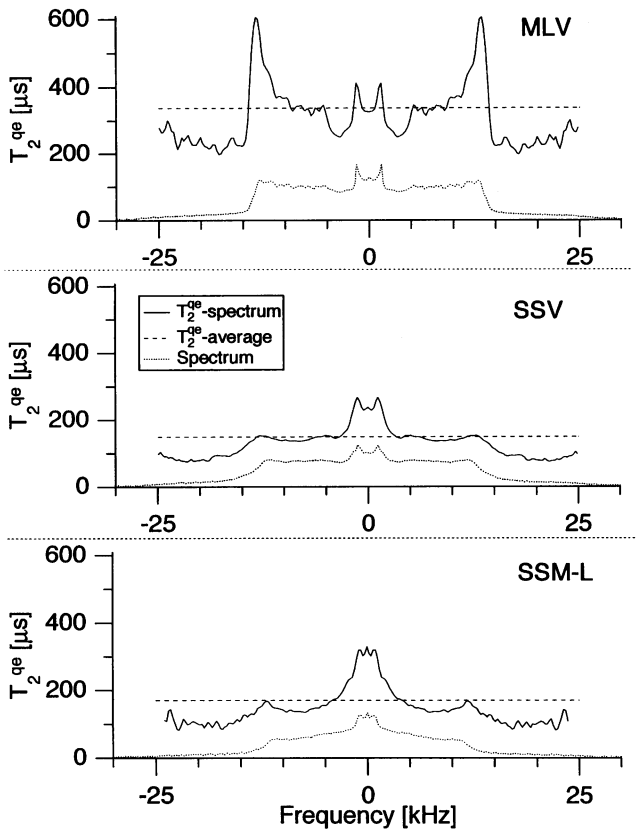

FIGURE 8 T_2^{qe} relaxation spectra of the MLV, SSV, and SSM-L samples for temperatures corresponding to the fluid phase of the samples (frequencies given in kHz). The solid line represents the T_2^{qe} spectra, the dotted line the conventional spectra, and the dashed horizontal line the average T_2^{qe} value. MLV, T = 43°C; SSV, T = 40°C; SSM, T = 44°C.

their T_m well above that of the bilayers systems, and its lower cooperativity and higher hysteresis is different from what is known for bilayers. Second, the depaked ^{2}H-NMR spectra of SSMs indicate that all DPPC-d_{62} undergo the same orientational ordering, in contrast to SSV systems (being comprised of two monolayers forming the bilayer) and the generalized order parameter profiles of the SSMs exhibit a different shape. Third, the temperature dependence of the transverse relaxation differs significantly for all three systems. Finally, the SSMs disperse in excess water homogeneously and without any tendency to aggregation, indicating that the silanized (hydrophobic) silica surface must be covered completely by a DPPC-d_{62} layer.

One possible explanation for the behavior of the SSM samples would be interdigitation of the lipid monolayer with the silane chains. Although we cannot rule out the occurrence of interdigitation we think it unlikely, as interdigitation normally does not occur in bilayers of saturated phosphatidylcholines with both lipid chains being of equal length and without the presence of a substance like an alcohol. The silane (C-18)/DMPC system should behave in the gel phase like a bilayer system and we do not see any force that would drive this system into an interdigitated state.

Our explanation for the behavior of the SSM samples is the following: for the MLV samples the area per lipid molecule can vary basically without constraint, which manifests itself in a 10–15% increase in molecular area in going through the main transition (Needham and Evans, 1988).

Due to the preparation procedure of the SSV samples the lipid area matches the surface area of the supporting silica beads in the fluid state of the bilayer. This leads to some tension in the gel state of the SSV bilayer, which removes the chain tilt of DPPC (Naumann et al., 1992), which for MLVs has a value of ~30° (Vaknin et al., 1991). The SSV bilayer may accommodate to the area reduction by the formation of pores or cracks, thereby acquiring lateral tension and exposing some (hydrophilic) silica surface to the water. This strain leads then to a reduction in the phase transition temperature for the SSV samples (Naumann et al., 1992).

During the preparation of the SSM samples (after the removal of the organic solvents) we cooled the silanized glass beads in the coating solution (still containing excess lipid) to temperatures below the main transition temperature of both MLV and SSM samples, before removal of the coating solution. We expect that lipid exchange will take place (the main transition temperature of the MLV samples being lower than that of the SSM samples) until the area of the SSM monolayer (in its gel state) matches approximately the area of the hydrophobic silane surface. The formation of pores or cracks, as hypothesized and observed (Sybille Bayerl, unpublished results) for SSVs above, cannot occur for the SSM samples, as the exposure of the highly hydrophobic silane surface to the water would result in a high cost in free energy. We expect, therefore, that the SSM monolayer in its gel state is either in a relaxed state or only under a slight amount of tension (due to the decreasing lipid exchange in going from the fluid to the gel state of the MLVs). This could lead to a small tilt of the SSM lipids in the gel phase.

During heating, the lipids within the monolayer are facing the problem of trying to prevent any contact between their hydrophobic regions or of the hydrophobic silane layer with water and at the same time of trying to achieve a 10–15% increase in their molecular area to undergo their main transition. This competition leads to an increase in the main transition temperature for the SSM samples.

At high enough temperatures the thermal energy is finally sufficient to allow excursions of the monolayer from the supporting silane layer. We expect the (reversible) local formation of surface ripples or small buds at the monolayer surface. Such structures can be expected to be highly curved, and consequently its lipids would undergo a motional averaging on the NMR time scale. This would explain the ^{2}H-NMR line shape of the SSM samples in the fluid phase (see spectra c3 and d3 in Fig. 4) that differs markedly from the bilayer spectra by a significant contribution of a narrow signal superimposing on the pake-doublet line shape.

From the fluid phase spectra in Fig. 4, one can estimate that ~10–15% of the lipids must be arranged in highly curved structures to account for the narrow signal, a value which is in excellent agreement with the increase in lipid area caused by the main transition. This reversible detachment of parts of the monolayer from the solid support could also be the reason why the generalized order parameter for fluid SSMs is lower than for fluid bilayers.

Addressing the question of the reason for the differences between the SSM-L and SSM-H samples we propose that the SSM-H samples have a significantly higher lipid density. This would explain the 5–6°C higher T_m of SSM-H, as the higher lipid density would increase the problem of the surface mismatch between the silane surface and the SSM monolayer in its fluid state. Preliminary results of fluorescence measurements using SSMs with fluorescence labeled lipids (Thomas Bayerl, unpublished results) show lower fluorescence intensities for the SSM-L samples and confirm this hypothesis.

A further support comes from film balance data as reported by Albrecht et al. (1978). They measured the isobars of a DPPC monolayer at the air/water interface, using a Langmuir film balance, at different values of the lateral pressure [see Fig. 1 *a* in Albrecht et al. (1978)]. Comparing the isobars for lateral pressures of π_l = 22.5 mN/m and π_l = 30.0 mN/m, respectively, we note that the T_m for the two pressures differs significantly and is ~4°C higher for the DPPC monolayer at the higher pressure of π_l = 30.0 mN/m. Moreover, the transition becomes more cooperative for higher π_l with a FWHM of ≈5°C at low and of ≈2°C at high pressure. These values and the difference in T_m are in qualitative agreement with those observed for the two SSM samples, as shown in the plot of M_1 versus temperature T in Fig. 3. It is also interesting to note that Albrecht et al. (1978) observed a hysteresis of T_m at π_l = 30 mN/m by measuring the isobars of DPPC monolayers in the ascendant and descendent temperature mode of 2–3°C, which is very similar to our value for the SSM-H sample.

The similarity of the T_2^{qe} relaxation time for SSV and SSMs in the fluid phase provides important information. Because the radii of the supports are identical and the lateral diffusion of the lipids has been shown to be the dominant T_2^{qe} relaxation contribution for fluid SSV (Dolainsky et al., 1993; Köchy, 1993), we can conclude that the diffusion constant of the SSM lipids must be similar to SSVs [measured by ^{2}H-NMR to be in the range $D_l = (4 \pm 0.5) \times 10^{-12}$ m^2 s^{-1} at 30°C (Köchy, 1993)]. This result seems reasonable considering that both the outer monolayer of the SSV and the SSM monolayer are in close contact with a similar fatty acid layer and the interlayer interaction force is in both cases solely the van der Waals attraction.

A surprising result is the difference in the temperature dependence of T_2^{qe} for SSV and SSMs. Fig. 7 shows that the decrease in T_2^{qe} from the gel to the fluid phase for SSMs is due to the extraordinarily high T_2^{qe} value of the gel state monolayer. In fact, this slow T_2^{qe} relaxation of the SSM in the gel state as compared to the bilayer systems is one of the major differences between the monolayer and bilayer systems from the dynamical point of view. We have no conclusive explanation for this high gel state T_2^{qe} of the monolayers, but can only suspect that this might be a consequence of the different lateral pressure in the monolayer compared to the bilayer.

The above results show that there is at least one step in the preparation of the SSMs that is crucial for the final lipid density in the supported monolayer. We suspect that the temperature at which the organic solvent evaporation is done might be decisive for the final lipid density in the SSM. This conclusion is drawn from the fact that only this temperature differed in the preparation of the two SSM samples, while all other parameters were identical. Further investigations will be required to establish whether a controlled temperature variation during the preparation can be employed to adjust a range of physically meaningful values for the lipid density in SSMs. This would open up new opportunities for a systematic study of monolayer properties using NMR and DSC.

CONCLUSIONS

Our results suggest that SSMs of DPPC are generally under a higher lateral pressure π_l in the fluid phase than the corresponding bilayer systems (supported and nonsupported) and that the lateral diffusion coefficient of the lipids in the fluid phase is similar for bilayers and monolayers. Moreover, the NMR data indicate remarkable differences between monolayers and bilayers regarding molecular order and some dynamical properties that affect the T_2^{qe} relaxation in the gel phase. The preparation technique of the SSM seems to offer the option to adjust the lipid density of the monolayer within a certain range and thus enables, for the first time, the ^{2}H-NMR spectroscopic study of lipid monolayers with the lipid density as a parameter.

We would like to thank Dr. Myer Bloom of the Department of Physics at the University of British Columbia for both his suggestions and the availability of time on his NMR-spectrometer, and Dr. Jenifer Thewalt for her helpful discussions.

The experimental work at the University of British Columbia was partially supported by an operating grant to Myer Bloom from the Natural Sciences and Engineering Research Council (NSERC) and by the Canadian Institute of Advanced Research (CIAR). Additional financial support came from grants from the Deutsche Forschungsgemeinschaft (SFB 266) and from the BMBF.

REFERENCES

Albrecht, O., H. Gruler, and E. Sackmann. 1978. Polymorphism of phospholipid monolayers. *J. Phys. Fr.* 39:301–313.

Bayerl, T. M., and M. Bloom. 1990. Physical properties of single phospholipid bilayers adsorbed to micro glass beads. *Biophys. J.* 58:357–362.

Bloom, M., C. Morrison, E. Sternin, and J. L. Thewalt. 1992. Spin echoes and the dynamic properties of membranes. *In* Pulsed Magnetic Resonance: NMR, ESR and Optics. D. M. S. Bagguley, editor. Clarendon Press, Oxford. 274–316.

Brumm, T., A. Möps, C. Dolainsky, S. Brückner, and T. M. Bayerl. 1992. Macroscopic orientation effects in broadline NMR-spectra of model membranes at high magnetic field strength. *Biophys. J.* 61:1018–1024.

Brumm, T., C. Naumann, E. Sackmann, A. R. Rennie, R. K. Thomas, D. Kanellas, J. Penfold, and T. M. Bayerl. 1994. Conformational changes of the lecithin headgroup in monolayers at the air/water interface. *Eur. Biophys. J.* 23:289–295.

Cresswell, J. P. 1994. Uniaxial ellipsometry of langmuir-blodgett films. *Langmuir.* 10:3727.

Davis, J. H. 1979. Deuterium magnetic resonance of the gel and liquid crystalline phases of dipalmitoyl phosphatidylcholine. *Biophys. J.* 27: 339–358.

Davis, J. H. 1983. The description of membrane lipid conformation, order and dynamics by ^{2}H-NMR. *Biochim. Biophys. Acta.* 737:117–171.

Dolainsky, C., A. Möps, and T. M. Bayerl. 1993. Transverse relaxation in supported and nonsupported phospholipid model membranes and the influence of ultraslow motions: a ^{31}P-NMR study. *J. Chem. Phys.* 98:1712–1720.

Fischer, B., M. Egger, S. Heyn, and H. Gaub. 1993. Antigen binding to a recognition pattern measured with surface plasmon microscopy. *Langmuir.* 9:136–140.

Fischer, A., and E. Sackmann. 1986. Electron microscopy and electron diffraction study of coexisting phases of pure and mixed monolayers transferred onto solid substrates. *J. Colloid Interface Sci.* 112:1–14.

Geib, G., W. Hickel, and D. Lupo. 1991. Ellipsometry on anisotropic langmuir-blodgett films. *Ber. Bunsen-Ges. Phys. Chem.* 95:1345.

Häussling, L., H. Ringsdorf, F. Schmidt, and W. Knoll. 1991. Biotin-functionalized self-assembled monolayers on gold: surface plasmon optical studies of specific recognition reactions. *Langmuir.* 7:1837–1837.

Helm, C. A., H. Möhwald, K. Kjaer, and J. Als-Nielsen. 1987. Phospholipid monolayers between fluid and solid state. *Biophys. J.* 52:381–390.

Hennion, M. C., C. Picard, and M. Caude. 1978. Influence of the number and length of alkyl chains on the chromatographic properties of hydrocarbonaceous bonded phases. *J. Chromatogr.* 166:21–35.

Huschilt, J. C., R. S. Hodges, and J. H. Davis. 1985. Phase equilibria in an amphiphilic peptide-phospholipid model membrane by deuterium nuclear magnetic resonance difference spectroscopy. *Biochemistry.* 24: 1377–1386.

Johnson, S. J., T. M. Bayerl, W. Weihan, H. Noack, J. Penfold, R. K. Thomas, D. Kanellas, A. R. Rennie, and E. Sackmann. 1991. Coupling of spectrin and polylysine to phospholipid monolayers studied by specular reflection of neutrons. *Biophys. J.* 60:1017–1025.

Kirkland, J. J. 1975. Microparticles with bonded phases for high-performance reverse-phase liquid chromatography. *Chromatographia.* 8:661–668.

Köchy, T. 1993. Bestimmung lateraler Diffusionskoeffizienten von Phospholipiden in festkörpergestützten Membranen mittels NMR-Relaxationsmethoden. Ph.D. thesis. Technische Universität München.

Lafleur, M., B. Fine, E. Sternin, P. R. Cullis, and M. Bloom. 1989. Smoothed orientational order parameter profile of lipid bilayers by ^{2}H-nuclear magnetic resonance. *Biophys. J.* 56:1037–1041.

Linseisen, F. M., J. L. Thewalt, M. Bloom, and T. M. Bayerl. 1993. ^{2}H-NMR and DSC study of SEPC-cholesterol mixtures. *Chem. Phys. Lipids.* 65:141–149.

Lösche, M., E. Sackmann, and H. Möhwald. 1983. A fluorescence microscopic study concerning the phase diagram of phospholipids. *Ber. Bunsen-Ges. Phys. Chem.* 87:848–852.

MacKay, A. 1981. A proton NMR moment study of the gel and liquid-crystalline phases of dipalmitoyl phosphatidylcholine. *Biophys. J.* 35: 301–313.

Malmsten, H. 1994. Ellipsometry studies of protein adsorption at lipid surfaces. *J. Colloid Interface Sci.* 168:247.

Miehlich, R., and H. E. Gaub. 1993. Holographic pattern photobleaching apparatus for the measurement of lateral transport processes at interfaces—design and performance. *Rev. Sci. Instrum.* 64:2632–2638.

Möhwald, H. 1990. Phospholipid and phospholipid-protein monolayers at the air/water interface. *Ann. Rev. Phys. Chem.* 41:441–476.

Möhwald, H. 1993. Surfactant layers at water surfaces. *Rep. Prog. Phys.* 56:653–685.

Morrow, M. R., J. P. Whitehead, and D. Lu. 1992. Chain-length dependence of lipid bilayer properties near the liquid crystal to gel phase transition. *Biophys. J.* 63:18–27.

Naumann, C., T. Brumm, and T. M. Bayerl. 1992. Phase transition behavior of single phosphatidylcholine bilayers on a solid spherical support studied by DSC, NMR, and FTIR. *Biophys. J.* 63:1314–1319.

Needham, D., and E. Evans. 1988. Structure and mechanical properties of giant lipid (DMPC) vesicle bilayers from 20°C below to 10°C above the liquid crystal-crystalline phase transition at 24°C. *Biochemistry.* 27: 8261–8269.

Nezil, F. A., C. Morrison, K. P. Whittall, and M. Bloom. 1991. Relaxation spectra in model membranes by deuterium nuclear magnetic resonance. *J. Magn. Reson.* 93:279–290.

Okamura, E., J. Umemura, and T. Takenaka. 1990. Orientation studies of hydrated DPPC multibilayers by polarized FTIR-ATR spectroscopy. *Biochim. Biophys. Acta.* 1025:94–98.

Putman, C., B. de Grooth, N. van Hulst, and J. Greve. 1992. A theoretical comparison between interferometric and optical beam deflection technique for the measurement of cantilever displacement in AFM. *Ultramicroscopy.* 42–44:1509–1513.

Rance, M., and R. A. Byrd. 1983. Obtaining high-fidelity spin-1/2 powder spectra in anisotropic media: phase-cycled Hahn echo spectroscopy. *J. Magn. Reson.* 52:221–240.

Reinl, H. M., and T. M. Bayerl. 1993. Interaction of myelin basic protein with single bilayers on a solid support: an NMR, DSC, and polarized infrared ATR study. *Biochim. Biophys. Acta.* 1151:127–136.

Reinl, H. M., and T. M. Bayerl. 1994. Lipid transfer between small unilamellar vesicles and single bilayers on a solid support: self-assembly of supported bilayers with asymmetric lipid distribution. *Biochemistry.* 33:14091–14099.

Rowe, E. S. 1983. Lipid chain length and temperature dependence of ethanol-phosphatidylcholine interactions. *Biochemistry.* 22:3299–3305.

Rowe, E. S. 1985. Thermodynamic reversibility of phase transitions. Specific effects of alcohols on phosphatidylcholines. *Biochim. Biophys. Acta.* 813:321–330.

Schmitt, F.-J., A. Weisenhorn, P. Hansma, and W. Knoll. 1992. Molecular recognition reactions at interfaces as seen by fluorescence, plasmon surface polaritons, and atomic force microscopy. *Thin Solid Films.* 210/211:666–669.

Sternin, E. 1985. Data acquisition and processing: a systems approach. *Rev. Sci. Instrum.* 56:2043–2049.

Sternin, E., M. Bloom, and A. L. MacKay. 1983. De-pake-ing of NMR spectra. *J. Magn. Reson.* 55:274–282.

Thomas, M., and H. Möhwald. 1994. Phospholipid monolayers at hydrocarbon/water interfaces. *J. Colloid Interface Sci.* 162:340–349.

Vaknin, D., K. Kjaer, J. Als-Nielsen, and M. Lösche. 1991. Structural properties of phosphatidylcholine in a monolayer at the air/water interface. *Biophys. J.* 59:1325–1332.

Wasserman, S. R., Y.-T. Tao, and G. M. Whitesides. 1989a. Structure and reactivity of alkylsiloxane monolayers formed by reaction of alkyltrichlorosilanes on silicon substrates. *Langmuir.* 5:1074–1087.

Wasserman, S. R., G. M. Whitesides, I. M. Tidswell, B. M. Ocko, P. S. Pershan, and J. D. Axe. 1989b. The structure of self-assembled monolayers of alkylsiloxanes on silicon: a comparison of results from ellipsometry and low-angle X-ray reflectivity. *J. Am. Chem. Soc.* 111: 5852–5861.

Zasadzinski, J. A., R. Viswanathan, L. Madsen, J. Garnaes, and D. K. Schwartz. 1994a. Langmuir-Blodgett films. *Science.* 263:1726–1733.

Zasadzinski, J. A., R. Viswanathan, D. K. Schwartz, J. Garnaes, L. Madsen, S. Chiruvolu, J. T. Woodward, and M. L. Longo. 1994b. Applications of atomic force microscopy to structural characterization of organic thin films. *Colloids Surfaces A.* 93:305–333.